1 **Assessment of anti-inflammatory bioactivity of extracellular vesicles is susceptible to error**

2 **via media component contamination**

3 Stephanie M. Kronstadt[1], Lauren Hoorens Van Heyningen[1], Amaya Aranda[1], Steven M. Jay[1, 2, *]

4

5 [1]Fischell Department of Bioengineering, University of Maryland, College Park, MD, 20742,

6 USA.

7 [2] Program in Molecular and Cell Biology, University of Maryland, College Park, MD, 20742,

8 USA.

9 *Corresponding author: Steven M. Jay, Ph.D., Fischell Department of Bioengineering,

10 University of Maryland, 3116 A. James Clark Hall, College Park, MD, 20742, USA, P: 301-405-

11 2829, F: 301-405-9953, smjay@umd.edu

12

13 Keywords: Exosome, bioreactor, size-exclusion chromatography, tangential flow filtration,

14 ultracentrifugation, contamination

15

16

17

18

19

20

Abstract:

Extracellular vesicles (EVs) are widely implicated as novel diagnostic and therapeutic modalities for a wide range of diseases. Thus, optimization of EV biomanufacturing is of high interest. In the course of developing parameters for a HEK293T EV production platform, we examined the combinatorial effects of cell culture conditions (i.e., static vs dynamic) and isolation techniques (i.e., ultracentrifugation vs tangential flow filtration vs size-exclusion chromatography) on functional characteristics of HEK293T EVs, including anti-inflammatory bioactivity using a well-established LPS-stimulated mouse macrophage model. We unexpectedly found that, depending on culture condition and isolation strategy, HEK293T EVs appeared to significantly suppress the secretion of pro-inflammatory cytokines (i.e., IL-6, RANTES) in the stimulated mouse macrophages. Further examination revealed that these results were most likely due to fetal bovine serum (FBS) EV contamination in HEK293T EV preparations. Thus, future research assessing the anti-inflammatory effects of EVs should be designed to account for this phenomenon.

42   **Introduction:**

43   With the potential to mirror the functional effects of parental cells and shuttle bioactive

44   cargoes intercellularly, extracellular vesicles (EVs) hold promise as early-stage biomarkers and

45   therapeutic interventions for various diseases as well as proficient drug delivery vehicles [1, 2].

46   As such, much effort has been expended in exploring the production, isolation, and functional

47   characterization of EVs resulting in various methodologies that differ vastly across individual

48   experiments and phases of research (i.e., preclinical vs clinical) [3]. In terms of EV production,

49   there has been a collective movement to implement dynamic and/or 3D cell culture

50   microenvironments, as these techniques are often more scalable than traditional flask culture and

51   can produce EVs that resemble those within the physiological niche [4]. Specifically, bioreactor-

52   based culture allows for the implementation of physiological parameters, including flow-derived

53   shear stress, and has been shown to significantly increase EV production across numerous

54   studies [5-14]. Importantly, the shift from static to dynamic culture is also known to cause

55   dramatic changes in the EV therapeutic profile [9, 12, 14-16]; in some cases elucidating EV

56   effects that were not present when utilizing traditional flask culture [15]. This phenomenon of

57   altered EV bioactivity can also be observed when implementing different EV isolation strategies

58   such as tangential flow filtration (TFF), ultracentrifugation (UC), or size-exclusion

59   chromatography (SEC) [16, 17]. Thus, optimizing EV production and isolation methods may be

60   vital in creating an ideal EV formulation for a given application.

61   Despite the important role that culture conditions and isolation strategies may play, only a

62   couple of studies have explored the combinatorial effects of these techniques on perceived EV

63   bioactivity [16, 18]. In one such study, Haraszti and colleagues demonstrated that EVs from

64   umbilical cord-derived MSCs cultured within a microcarrier-based bioreactor and isolated via

65   TFF were more efficient in delivering functional therapeutic siRNA into neurons than those EVs

66   isolated from the same bioreactor culture using UC. They also show that bioreactor EVs isolated

67   using UC were no more effective in siRNA transfer than EVs from traditional flask culture

68   isolated using UC or TFF [16]. Previous research also cautions over assuming that the EVs are

69   solely responsible for therapeutic activity, as many isolation strategies can result in the co-

70   isolation of process impurities [19]. Demonstrating this is a study by Whitaker et al. in which the

71   co-isolated and non-EV associated VEGF within MSC EV preparations had pro-angiogenic and

72   pro-migratory effects on endothelial cells that could wrongfully be accredited to the EVs [20].

73   Altogether, these studies emphasize the importance of optimizing both cell culture conditions

74   and isolation methods simultaneously while implementing careful functional assessment to

75   produce the most viable EV therapeutic platform.

76   As for functional evaluation of EVs, much interest is often paid to EV anti-inflammatory

77   capacity, as inflammatory dysregulation is ubiquitous in many chronic diseases (e.g., sepsis,

78   cancer, and autoimmune disorders) and tissue regeneration issues [21, 22]. Recently, Pacienza

79   and colleagues developed an *in vitro* LPS-stimulated mouse macrophage assay to assess the anti-

80   inflammatory potential of mesenchymal stem cell (MSC)-derived EVs. Notably, results obtained

81   in this *in vitro* assay were able to predict the efficacy of different MSC EV preparations in

82   suppressing LPS-stimulated inflammation in mice [23]. As such, this assay and derivatives of it

83   have been used regularly to test the anti-inflammatory properties of EVs [24-26].

84   In the present investigation, we examined the combinatorial effects of cell culture

85   conditions (i.e., static vs dynamic) and isolation techniques (i.e., UC vs TFF vs SEC) on the size,

86   morphology, and functional characteristics of EVs from HEK293T cells – a highly scalable

87   source for the production of therapeutic EVs [27]. Surprisingly, depending on culture condition

4

88 and isolation strategy, HEK293T EVs appeared to exert immunosuppressive effects in an LPS-

89 stimulated mouse macrophage model. We found that this result was most likely due to FBS EV

90 contaminants within the HEK293T EV samples. Our results highlight the importance of

91 recognizing and controlling for potential contaminants in EV preparations when utilizing this

92 assay.

93

94 **Methods:**

95 Cell Maintenance

96   Human embryonic kidney cells (HEK293T) were purchased from ATCC (CRL-3216)

97 and cultured in T175 flasks using Dulbecco's Modification of Eagle's Medium (DMEM) [+] 4.5

98 g/L glucose, L-glutamine, and sodium pyruvate (Corning, 10-013-CV) supplemented with 10%

99 fetal bovine serum (FBS; VWR, 89510-186) and 1% penicillin-streptomycin (P/S; Corning, 30-

100 002-CI). All HEK293T cells used in experiments were between passages 4-7. RAW264.7 mouse

101 macrophages (ATCC, TIB-71) were cultured in T175 flasks with DMEM [+] 4.5 g/L glucose, L-

102 glutamine, and sodium pyruvate (Corning, 10-013-CV) supplemented with 5% FBS and 1% P/S.

103 RAW264.7 at passages 10-13 were used in experiments. Human umbilical vein endothelial cells

104 (HUVECs) pooled from multiple donors (PromoCell; C-12203) were cultured in T75 flasks

105 coated with 0.1% gelatin at 37 °C for 1 h prior to seeding. HUVECs were maintained in complete

106 endothelial growth medium-2 (EGM2; PromoCell, C-22111) supplemented with 1% P/S. During

107 experiments, HUVECs were cultured in endothelial basal medium-2 (EBM2; PromoCell, C-

108 22221) supplemented with 0.1% FBS and 1% P/S. HUVECs at passages 3 and 4 were used in

109 experiments.

110

111   HEK293T Cell Culture Conditions

112   *Flask and Scaffold Culture*

113   As static controls, HEK293T cells were cultured within T75 tissue culture flasks (VWR,

114   BD353136) or a 3D-printed scaffold. The scaffold was printed from a biocompatible acrylate-

115   based material (E-Shell 300; EnvisionTEC) using an EnvisionTEC Perfactory 4 Mini Multilens

116   stereolithography apparatus (EnvisionTEC, Inc., Dearborn, MI, USA). The 12 cm^3 volume

117   construct contained a growth surface area (50 cm^2) with small pillars (1 mm in diameter) that

118   were spaced 2.5 mm apart. This design allowed efficient cell removal and immunofluorescence

119   imaging as well as the facilitation of nutrient and gas transport and a mechanism to control fluid

120   parameters predictably. Following printing, scaffolds were submerged in 99% isopropanol

121   (Pharmco-Aaper, Shelbyville, KY) for 5 min to remove excess resin. The scaffolds were then

122   flushed with fresh 99% isopropanol until all excess resin was removed after which the scaffolds

123   were dried with filtered air. Resin curing was accomplished using 2,000 flashes of broad-

124   spectrum light (Otoflash, EnvisionTEC, Inc.). Scaffolds were then cleaned in 100% ethanol for

125   >30 min to eliminate any remaining contaminants, after which they were placed in fresh 100%

126   ethanol and sterilized in an ultraviolet sterilizer (Taylor Scientific, 17-1703) for 10 min.

127   Rehydration was achieved by soaking the scaffolds in sterile serial dilutions of ethanol to 1X

128   PBS (pH 7.4) for 5 minutes per step (75:25, 50:50, 25:75, 0:100 ethanol:PBS). Rehydrated

129   scaffolds were placed in 100% sterile 1X PBS in at 4°C until use. When ready to use, scaffolds

130   were coated with 3 µg/cm^2 fibronectin in sterile water at 37°C for 30 min. Flasks and scaffolds

131   were seeded at a density of 2,500 cell/cm^2 in 15 mL of media.

132

133

134 *Perfusion Bioreactor Culture*

135   For the perfusion bioreactor condition, select seeded scaffolds were hooked up to a

136 Masterflex L/S Digital Peristaltic Pump (Cole-Parmer; Vernon Hills, IL, USA) using platinum-

137 cured silicon tubing (Cole-Parmer, EW-95802-04). The scaffolds were operated at a flow rate of

138 5 mL/min which corresponded to a shear stress value of 3×10^{-3} dyn/cm^2 as determined previously

139 by computational fluid modeling via the Flow Simulation add-in for SolidWorks (Dassault

140 Systèmes, Velizy-Villacoublay, France). The set-up allowed the scaffolds to be connected to a

141 media reservoir containing 50 mL of EV-depleted FBS media. The pump and scaffolds were

142 then placed within a cell culture incubator at 37°C with 5% CO_2.

143

144 Cell Staining and Imaging

145   After 24 h culture in the bioreactor, the scaffolds were filled with 4% paraformaldehyde

146 for 15 min at room temperature to fix the HEK293T cells. Scaffolds were then washed three

147 times with 1X PBS and filled with permeabilization buffer (300 µM sucrose, 100 µM sodium

148 chloride, 6 µM magnesium chloride, 20 µM HEPES, and 0.5% Triton-X-100 solution) for 5 min

149 at room temperature. AlexaFluor 488 Phalloidin in PBS (1:100) was used to stain cell actin and

150 cells were visualized on a Nikon Ti2 Microscope (Nikon, Minato City, Tokyo, Japan).

151

152 Media EV-Depletion Protocols

153   To produce EV-depleted FBS, heat-inactivated FBS was centrifuged at $118,000 \times g$ for

154 16 h and the resulting supernatant was filtered through a 0.2 µm bottle top filter for use in

155 subsequent media supplementation. To produce EV-depleted whole media, DMEM with full

156   supplementation (10% heat-inactivated FBS and 1% P/S) was centrifuged at $118,000 \times g$ for 16

157   h and the supernatant was sterile filtered (0.2 μm) for direct use in ensuing experiments.

158

159   EV Isolation Techniques

160   During experiments, HEK293T culture media was replaced with media made with 10%

161   EV-depleted FBS and 1% P/S (i.e., EV-depleted FBS media) or EV-depleted whole media.

162   Approximately 100 mL of HEK293T conditioned media from each culture condition (i.e., flask,

163   scaffold, or bioreactor) was subjected to a series of differential centrifugation to clear the media

164   of cells as previously described [28]. In brief, conditioned media was first centrifuged at $1,000 \times$

165   g for 10 min to remove any cells that may have detached during collection. The supernatant was

166   then collected and centrifuged at $2,000 \times g$ for 20 min to remove any larger cellular debris. This

167   supernatant was then centrifuged at $10,000 \times g$ for 30 min to remove any large organelles

168   remaining. The cleared conditioned media was then subjected to the various isolation techniques

169   described below. Final EV samples were stored at 4°C and were analyzed within three days of

170   collection.

171

172   *Ultracentrifugation*

173   For ultracentrifugation (UC), the conditioned media was subjected to an additional

174   centrifugation step of $118,000 \times g$ for 2 h in a Type 70 Ti ultracentrifuge rotor (Beckman

175   Coulter). The resulting EV pellet was resuspended in 1X PBS and placed into a Nanosep 300

176   kDa MWCO spin column (Pall, OD300C35) and spun at $8,000 \times g$ until all PBS filtered through

177   the membrane (~10-12 min). EVs were washed two more times with 1X PBS, resuspended in 1X

178   PBS, and sterile filtered using a 0.2 μm syringe filter.

179   *Tangential Flow Filtration*

180   Tangential flow filtration (TFF) was performed using a KrosFlo KR2i TFF system

181 (Spectrum Labs, Los Angeles, CA, USA) equipped with a 100 kDa MWCO hollow fiber filter

182 comprised of a modified polyethersulfone membrane (Spectrum Labs, D02-E100-05-N). Prior to

183 processing the cleared conditioned media, the filter was first washed with at least three volumes

184 of 1X PBS to remove the bacteriostatic reagent. Each filter was used no more than five times. To

185 keep a shear rate at 4000 s^{-1}, the flow rate was kept constant at 106 mL/min. All samples were

186 processed at a transmembrane pressure (TMP) of 5 psi. Samples were first concentrated to a

187 volume of 25 mL and then diafiltrated five times in 1X PBS to exchange buffers. Following

188 buffer exchange, the EVs were concentrated to a volume of 6-9 mL. Further concentration was

189 performed using a 100 MWCO centrifugal concentrator (Corning, 431486) to achieve a final

190 volume of ~0.5 mL. The final EV suspension was sterile filtered using a 0.2 μm syringe filter.

191

192   *Size-Exclusion Chromatography*

193   EVs were isolated via size-exclusion chromatography (SEC) using qEV Original columns

194 (Izon Science, ICO-35) per the manufacturer's protocol. Briefly, the cleared conditioned media

195 was concentrated to 0.5 mL using the TFF set-up and centrifugal concentrators described in the

196 previous section. After flushing the columns with 1X PBS, 500 μl of the concentrated media was

197 applied to the top of the column and the first four 0.5 mL fractions after the void volume were

198 collected and pooled. The pooled fractions were then concentrated using 100 MWCO centrifugal

199 concentrators to 0.5 mL and sterile filtered (0.2 μm).

200

201

202   Media Testing

203   To assess the effects of media components, various media formulations were subjected to

204   the aforementioned isolation techniques. Unconditioned media test formulations (i.e., media

205   without exposure to cells) were defined as the following: no cell (media without any cell

206   conditioning), + FBS (media supplemented with EV-depleted FBS), or -FBS (media without

207   FBS). To evaluate the effects of EV-depletion protocols used to remove contaminating EVs from

208   the FBS components, HEK293T cells cultured in flasks were exposed to either EV-depleted FBS

209   media or EV-depleted whole media as previously described (see Media EV-depletion Protocols

210   section).

211

212   EV Characterization

213   *Protein and Particle Quantification*

214   Total protein concentration was determined using BCA methods (G-Biosciences, 786-

215   571) and size distribution as well as particle concentration were assessed using a NanoSight

216   LM10 (Malvern Instruments; Malvern, UK) with Nanoparticle Tracking Analysis (NTA)

217   software version 2.3. For each sample, three 30-second videos were captured with a camera level

218   set at 12. EV samples were diluted to obtain 20-100 particles per frame and at least 200

219   completed tracks per video to ensure accurate analysis. The detection threshold was set and kept

220   constant across all replicates and samples. The total number of EVs was evaluated using the final

221   resuspension volume and then divided by the number of cells to give final data expressed as total

222   number of EVs per cell.

223

224

EV Markers

Western blot analysis was used to determine the presence of specific EV markers as well as the purity of each sample. Based on the BCA results, 7 μg of protein from each EV sample was used for analysis and compared with 7 μg of cell lysate. EV markers were assessed using primary antibodies for Alix (Abcam, ab186429), TSG101 (Abcam, ab125011), and CD63 (Proteintech, 25682-1-AP), while the absence of contaminating proteins were confirmed using antibodies for GAPDH (Cell Signaling Technology, 2118) and calnexin (Cell Signaling Technology, 2679). All primary antibodies were added at a 1:1,000 dilution, excluding GAPDH which was diluted 1:2,000. A 1:10,000 dilution of a goat anti-rabbit secondary (LI-COR Biosciences, 926-32211) was used. Protein bands were imaged using a LI-COR Odyssey CLX Imager and analyzed using the associated software.

Transmission Electron Microscopy

EV morphology was visualized via transmission electron microscopy (TEM) using a negative staining technique. A portion of each EV sample (10 μl) was fixed in a 1:1 solution using 4% EM-grade paraformaldehyde (Electron Microscopy Sciences, 157-4-100) for 30 min at room temperature. A 10 μl droplet of the EV-PFA mixture was then allowed to adsorb to a carbon-coated copper grid (Electron Microscopy Sciences, CF200-Cu-25) for 20 min. After a brief wash using a of a drop of 1X PBS, the EV-coated grid was then placed on a drop of 1% glutaraldehyde (in 1X PBS) for 5 min. The grid was washed 5-7 times (2 min each wash) on deionized water droplets with blotting on filter paper between washes. The grid was then positioned on a droplet of uranyl-acetate replacement stain (Electron Microscopy Sciences,

247   22405) and allowed to dry completely for 10 min. Once prepared, the grids were imaged at 200

248   kV on a JEOL JEM 2100 LaB6 TEM.

249   Bioactivity Assessment

250   *Macrophage Stimulation Assay*

251   To assess the effects of EV isolation technique and culture method on downstream

252   applications, a mouse macrophage stimulation assay was utilized [23, 29]. RAW264.7 mouse

253   macrophages were seeded at 60,000 cells/well in triplicate in a 48-well plate. 24 h later, two

254   groups (i.e., six wells) of the macrophages were pre-treated with just media with PBS (vehicle

255   control). Another group was pretreated using media supplemented with dexamethasone at 1

256   μg/mL (resuspended in 1X PBS) which served as the positive control (Dex; Sigma-Aldrich,

257   D4902-25 MG). The remaining macrophages were pre-treated with the HEK293T EVs

258   (resuspended in 1X PBS) from the various culture and isolation techniques at 5E9 EVs/mL

259   diluted in cell culture media. After 24 h of incubation, the pre-treatments were removed and the

260   macrophages were washed once with sterile 1X PBS. Cells were then either treated with just

261   media spiked with PBS (vehicle control) or media spiked with lipopolysaccharide at 10 ng/mL

262   (LPS; resuspended in 1X PBS; Sigma-Aldrich, L4391-1MG) for 4 h. The supernatants were then

263   collected from the RAW264.7 macrophages and frozen at -80° C. Levels of secreted IL-6,

264   RANTES, and TNF-α were assessed using the appropriate DuoSet ELISA kit (R&D Systems,

265   DY406, DY478, DY410).

266

267   *Tube Formation Assay*

268   HUVECs were used to evaluate effects on endothelial tube formation as previously

269   described [30]. In brief, HUVECs were trypsinized, counted, and aliquoted into a tube marked

12

270   for each treatment that was filled with 2 mL of EBM2 supplemented with 0.1% FBS and 1% P/S.

271   The cells were then pelleted at $220 \times g$ after which the supernatant was removed and the cells

272   were aliquoted to a final concentration of 120,000 cells/mL into complete growth media (positive

273   control), basal media (EBM2 plus 0.1% FBS and 1% P/S) devoid of EVs (negative control), or

274   basal media supplemented with EVs (5E9 EVs/mL) and gently but thoroughly resuspended. The

275   treatments were then applied in triplicate at 500 μl per well (i.e., 60,000 cells/well) in a 24-well

276   plate coated with growth factor reduced Matrigel (Corning, 354230). Cells were imaged at 6 h

277   using a Nikon Eclipse Ti2 Microscope and the number of loops formed by the HUVECs was

278   quantified using ImageJ.

279

280   *Gap Closure Assay*

281   To assess endothelial migration, HUVECs were seeded at 15,000 cells/well in a 0.1%

282   gelatin-coated 96-well plate and allowed to grow to confluency. The monolayer was then

283   disrupted using an AutoScratch (BioTek Instruments; Winooski, VT, USA) to create a cell gap

284   meant to simulate a wound. HUVECs were gently washed with 1X PBS and serum-starved for 2

285   h via incubation with basal media. Following serum starvation, the media was aspirated and

286   replaced with complete growth media (positive control), basal media (negative control), or basal

287   media spiked with EVs (5E9 EVs/mL). The cell gap was imaged at 0 h and 20 h using a Nikon

288   Eclipse Ti2 Microscope and the change in the gap area was calculated using ImageJ as

289   previously described [31].

290
291   Statistics

292   Data are presented as mean ± standard error of the mean (SEM). Two-way ANOVAs

293   with Tukey's multiple comparisons tests were used to determine statistical differences ($p < 0.05$)

13

294   among groups across cell culture conditions and EV isolation techniques in the *in vitro*

295   stimulated macrophage assay. One-way ANOVAs with Tukey's multiple comparisons tests were

296   used to detect statistical differences ($p < 0.05$) among groups in the *in vitro* gap closure assay and

297   tube formation assay. All statistical analyses were performed using Prism 9.1 (GraphPad

298   Software, La Jolla, CA). Notation for significance in figures are as follows: ns – $p > 0.05$: *- $p <$

299   0.05; ** - $p < 0.01$; *** or ### - $p < 0.001$; **** or ####- $p < 0.0001$).

300

301   **Results:**

302   *Cell culture condition and EV isolation technique have no effect on EV size or morphology*

303   As various factors including cell culture methods and isolation techniques have been

304   shown to influence downstream EV efficacy [32], we set out to dissect the effect of these factors

305   on HEK293T EVs. HEK293T cells were chosen based on their proven ability to be integrated

306   into scalable biotech processes as well as demonstrated ability to be engineered for therapeutic

307   EV production [27, 33]. The EVs that they secreted are also thought to be relatively

308   therapeutically inert, especially when compared with the EVs of other cell types (e.g.,

309   mesenchymal stem cells; MSCs) [34-36]. Thus, analysis of HEK293T EVs in biological assays

310   could reveal confounding factors in commonly used EV production and characterization

311   strategies. In the current study, HEK293T cells were cultured in a 3D-printed, acrylate-based

312   scaffold hooked up to a peristaltic pump and operated at a 5 mL/min flow rate ($3x10^{-3}$ dyn/cm^2),

313   constituting a set-up which will be referred to as the bioreactor. Prior studies in our lab have

314   revealed that this specific flow rate allows adequate cell viability and increases EV production

315   (i.e., EVs per cell) [5]. HEK293T cells were also cultured in static scaffolds and T75 flasks as

316   controls. Conditioned media from the various culture methods were collected and EVs were

317   isolated via ultracentrifugation (UC), tangential flow filtration (TFF), or size exclusion

318   chromatography (SEC) as depicted in **Figure 1A**. There were no significant alterations in EV

319   mode size as measured by NTA (Flask UC – 96.9 ± 5.5 nm; Flask TFF – 86.3 ± 6.4 nm; Flask

320   SEC – 90.9 ± 10.1 nm; Scaffold UC – 88.8 ± 6 nm; Scaffold TFF – 92.9 ± 3.4 nm; Scaffold SEC

321   – 90.9 ± 9.5 nm; Bioreactor UC – 98.7 ± 5.6 nm; Bioreactor TFF – 84.2 ± 4 nm; Bioreactor SEC

322   – 90.1 ± 2 nm) (**Figure 1B**). Additionally, greater than 90% of the EV population from each

323   sample were well within the range of acceptable exosomal diameter (40 – 200 nm) (**Figure 1B**)

324   (Andaloussi et al. 2013). Immunoblotting established the presence of specific EV markers (Alix,

325   TSG101, and CD63) and the absence of cellular debris indicators (Calnexin and GAPDH)

326   (**Figure 1C**). TEM images showed no effect of culture or isolation technique on HEK293T EV

327   morphology (**Figure 1D**).
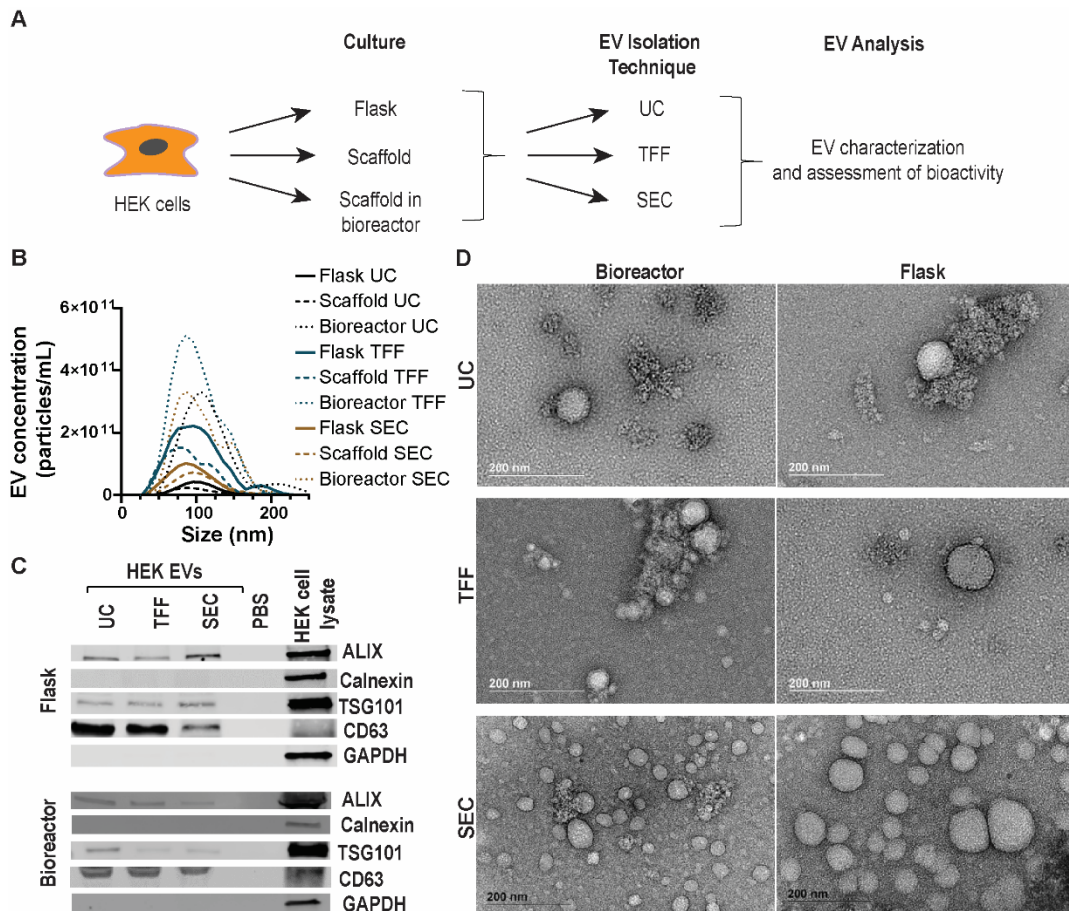
Figure 1. Culture conditions and isolation techniques do not impart significant effects on size or morphology of HEK293T EVs. (A) Schematic depicting the experimental workflow. (B) Size distribution of HEK293T-derived EVs generated and isolated via the various culture conditions and isolation methods (ultracentrifugation, UC; tangential flow filtration, TFF; size exclusion chromatography, SEC). (C) Immunoblotting of HEK293T EVs from flask and bioreactor conditions isolated via UC, TFF, or SEC for EV-specific markers (CD63, Alix, TSG101) and cell markers (Calnexin and GAPDH). (D) TEM images of HEK293T EVs isolated from the flask and bioreactor culture conditions using each isolation method. Data and images are representative of two independent experiments (N = 2).

Immunomodulatory activity of HEK293T EV preparations is altered by culture condition and

isolation method

HEK293T EV isolates prepared using the various culture conditions (i.e., flask, scaffold, or bioreactor) and separation methods (i.e., UC, TFF, or SEC) were assessed in an LPS-

16

344   stimulated mouse macrophage assay, with final read-outs being the secretion levels of several

345   inflammatory cytokines (i.e., IL-6, RANTES, TNF-α). These cytokines are known to regulate

346   inflammation and are correlated with EV immunomodulatory activity *in vivo* [23, 37, 38]. It was

347   observed that levels of the secreted inflammatory cytokines differed significantly when

348   macrophages were exposed to HEK293T EV preparations from the various culture methods and

349   isolation technique combinations (**Figure 2**). For every cytokine analyzed, there was a

350   significant interaction of culture technique with isolation method as determined by a two-way

351   ANOVA (IL-6: $p < 0.0001$; RANTES: $p < 0.0001$; TNF-α: $p = 0.0056$). Surprisingly, Tukey's

352   multiple comparison tests revealed that HEK293T EV preparations from every condition, except

353   those from the bioreactor culture isolated using SEC, significantly reduced the levels of IL-6

354   secretion compared with the LPS-only group (**Figure 2A**). A similar trend, although not always

355   significant, was observed in the levels of secreted RANTES (**Figure 2B**). Isolating via the UC

356   method in particular produced preparations with a significantly increased ability to suppress the

357   secretion of inflammatory cytokines (**Figure 2**); an effect that was often lost if cells were

358   cultured within the bioreactor (**Figure 2B, C**). Notably, preparing EV isolates via TFF or SEC

359   weakened the observed suppression of cytokine secretion.

360
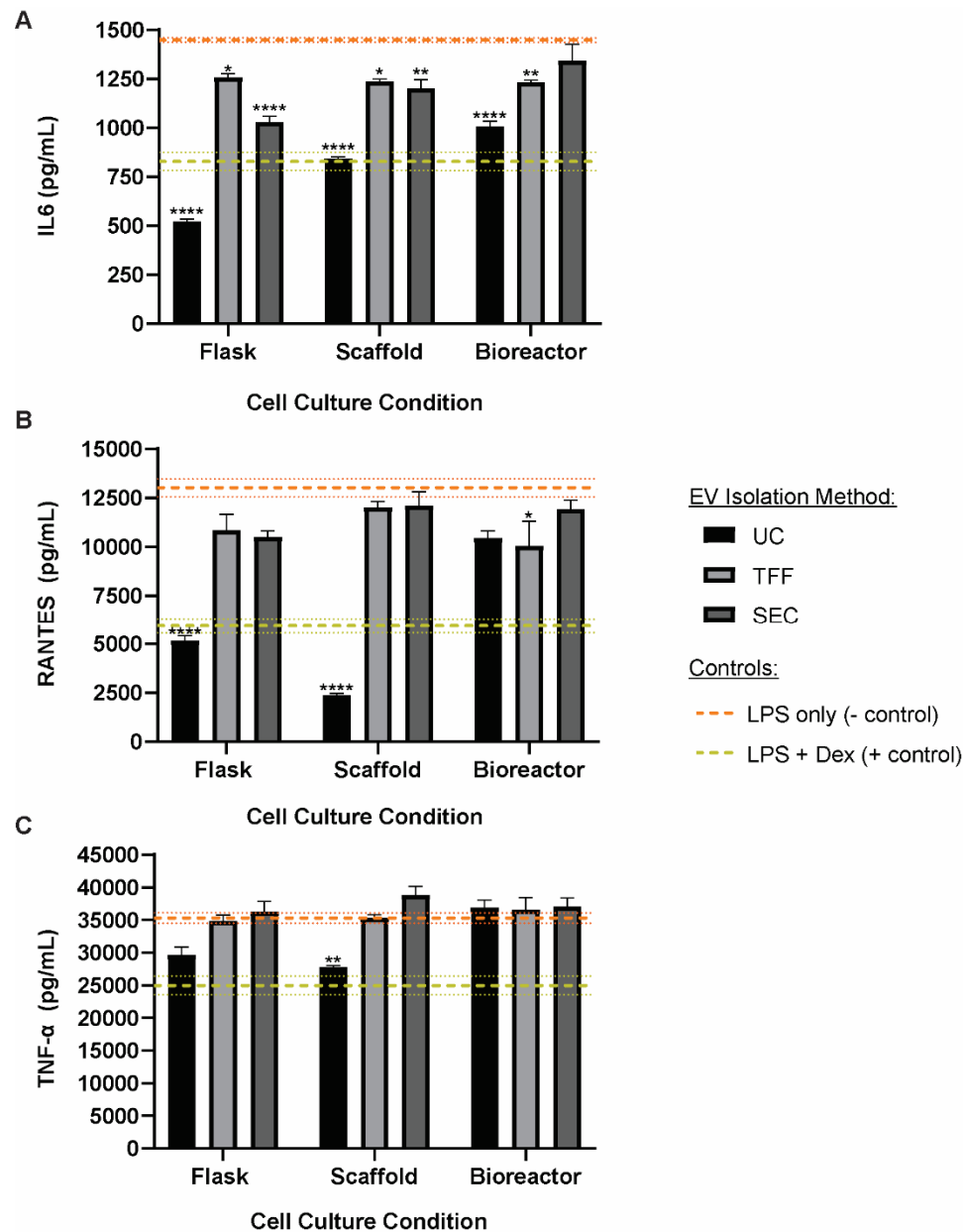
Figure 2. Culture conditions and isolation techniques alter the immunomodulatory activity of HEK293T EVs. RAW264.7 mouse macrophages were pretreated with either HEK293T EVs from cells within the various culture conditions (i.e., flask, scaffold, or perfusion bioreactor) and isolated using different techniques (i.e., ultracentrifuge – UC, tangential flow filtration – TFF, or size-exclusion chromatography – SEC) or with dexamethasone (Dex) prior to stimulation with lipopolysaccharide (LPS). RAW264.7 supernatants were collected and (A) IL-6, (B) RANTES, and (C) TNF-α secretion was quantified via ELISAs. Data is plotted as mean and error bars represent the standard error of the mean (SEM). Control means are represented as dashed lines with dotted lines representing the SEM. Data includes three technical replicates and data are representative of two independent biological replicates (N = 2). Statistical significance was

18

372 calculated using a two-way ANOVA using Tukey's multiple comparison tests (*- $p < 0.05$; ** -

373 $p < 0.01$; **** - $p < 0.0001$ compared to LPS negative control).

374

375

376 *Media components influence the results of the macrophage stimulation assay*

377 To determine if media components affect the readout of the macrophage stimulation

378 assay, unconditioned media (i.e., media not previously exposed to HEK293T cells) and

379 conditioned media collected from HEK293T cells cultured in flasks were exposed to the various

380 isolation techniques (i.e., UC, TFF, or SEC) and applied to RAW264.7 macrophages prior to

381 LPS stimulation. Interestingly, both unconditioned and conditioned media preparations

382 significantly and similarly reduced the secretion of IL-6 from the stimulated macrophages

383 regardless of isolation technique (**Figure 3A**). Analysis of RANTES concentrations reveals a

384 reduction of the cytokine only in the cells treated with the UC-isolated preparations, with a

385 significant reduction in RANTES secretion when treated with the conditioned media (**Figure**

386 **3B**). However, when looking at TNF-α, the trends readily apparent in the IL-6 concentrations

387 were lost, except for a reduction when isolating with TFF (**Figure 3C**).

388

389
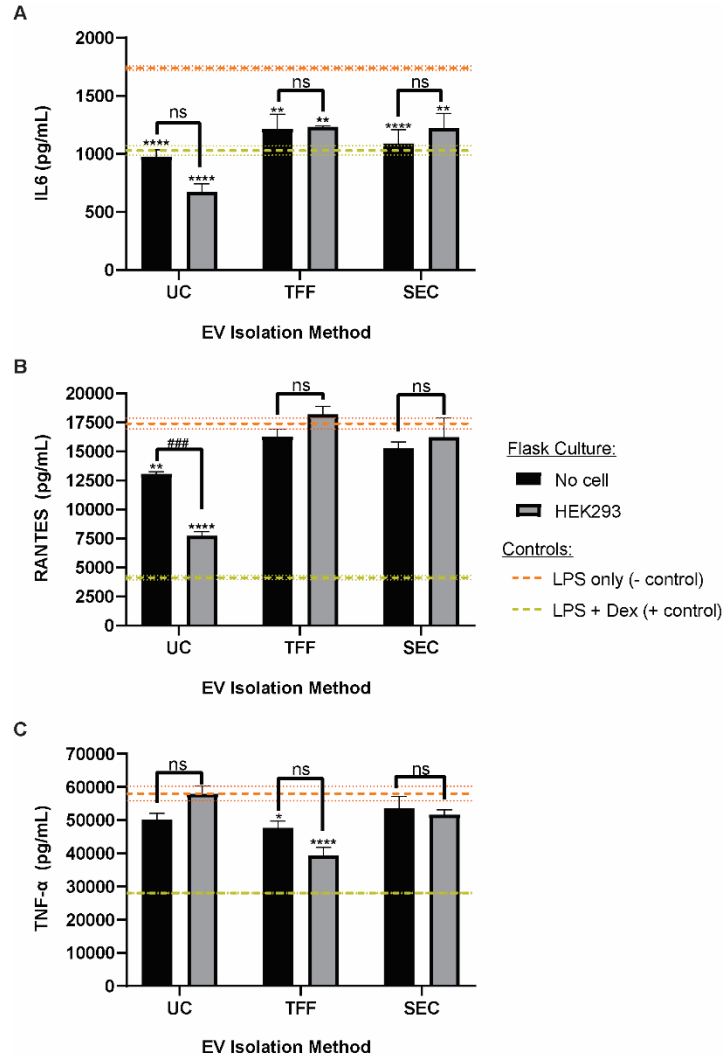
Figure 3. Unconditioned media subjected to each isolation technique alter cytokine secretion in stimulated macrophages in a similar manner to HEK293T EV preparations.
Unconditioned media (i.e., no prior exposure to cells; 'no cell') or media conditioned with HEK293T cells within flasks were exposed to each isolation procedure (i.e., ultracentrifugation – UC, tangential flow filtration – TFF, or size-exclusion chromatography – SEC). Either the resulting preparations or dexamethasone (Dex) were applied to RAW264.7 mouse macrophages prior to stimulation with lipopolysaccharide (LPS). RAW264.7 supernatants were collected and (A) IL-6, (B) RANTES, and (C) TNF-α secretion was quantified via ELISAs. Data is plotted as mean and error bars represent the standard error of the mean (SEM). Control means are represented as dashed lines with dotted lines representing the SEM. Data includes three technical replicates and data are representative of two independent biological replicates (N = 2). Statistical significance was calculated using a two-way ANOVA using Tukey's multiple comparison tests (ns – p > 0.05; *- p < 0.05; ** - p < 0.01; **** - p < 0.0001 compared to LPS negative control).

20

406   To determine if these results were confined to the stimulated macrophage assay,

407   unconditioned media were isolated via UC and applied in two orthogonal *in vitro* assays. Results

408   showed that in both an endothelial gap closure assay and an endothelial tube formation assay,

409   unconditioned media did not induce any significant response and were similar to the negative

410   control (i.e., basal media) (**Figure 4**).

411

412
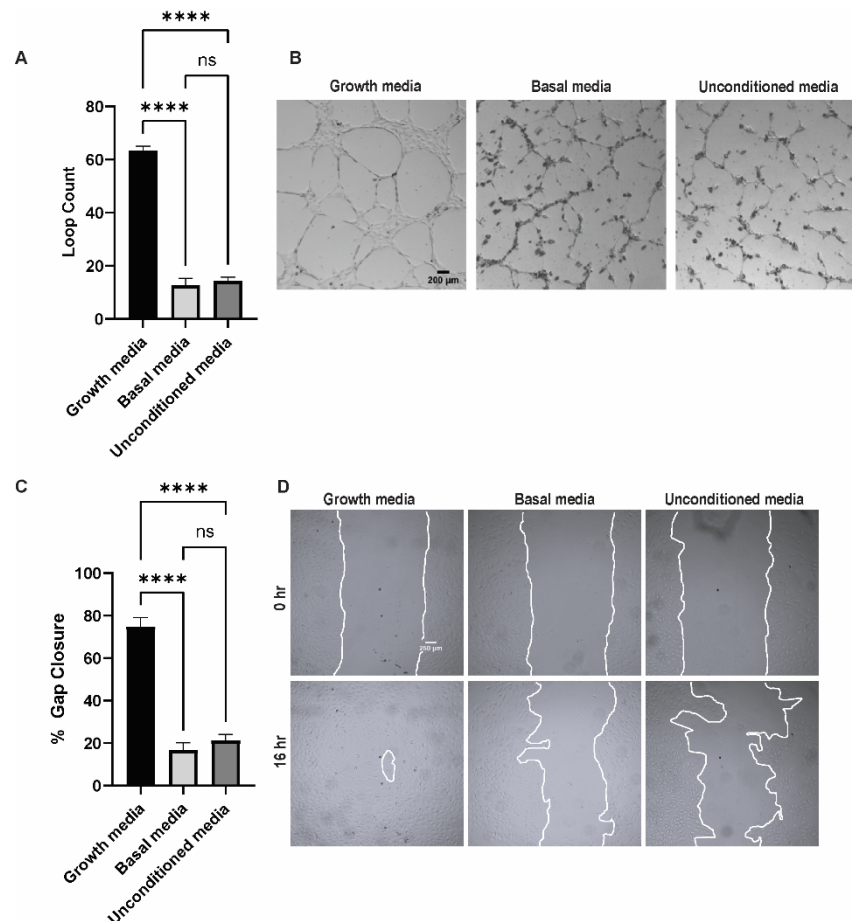
Figure 4. Unconditioned media do not elicit any significant response in *in vitro* angiogenic assays. (A) Number of loops formed by human umbilical vein endothelial cells (HUVECs) in a tube formation assay after treatment with growth media (positive control), basal media (negative control), or unconditioned media following exposure to the ultracentrifugation isolation protocol along with (B) the corresponding representative images at 16 hr. (C) Percent gap closure 16 h after treatment with growth media, basal media, or unconditioned media subjected to ultracentrifugation. There were no significant differences between the unconditioned media treatment and the negative control (basal media) in either assay ($p > 0.05$). All images and data are representative of two biological replicates with three technical replicates each. Statistical

21

422 differences were analyzed using a one-way ANOVA with Tukey's multiple comparisons test (ns
423 – p > 0.05, **** - p < 0.0001).
424
425   To further dissect the observed effects, unconditioned media containing FBS (i.e., + FBS)

426 or unconditioned media without FBS (i.e., - FBS) underwent the UC isolation protocol and were

427 tested in the stimulated macrophage assay. The results revealed that the suppression of IL-6

428 secretion from macrophages was lost when FBS was absent from the media (**Figure 5A**). A

429 similar trend was observed when looking at RANTES levels, but only when using the UC

430 isolation method (**Figure 5B**). All patterns of cytokine suppression were diminished when

431 examining TNF-α levels (**Figure 5C**). Based on these results, the EV-depletion protocols for

432 media supplementation were examined. Two disparate protocols were followed, and the media

433 tested again in the macrophage assay. In brief, FBS was either depleted of EVs prior to addition

434 into the media (i.e., FBS-depleted) or after being added to the media (i.e., whole media-

435 depleted), subjected to the UC isolation protocol, and applied to macrophages prior to LPS

436 stimulation. Results showed that when whole media was depleted, the secretion of IL-6 from

437 stimulated mouse macrophages was no longer subdued and was statistically similar to the LPS-

438 only control (**Figure 6**).

439

440

441

442

443

444

445

446

447
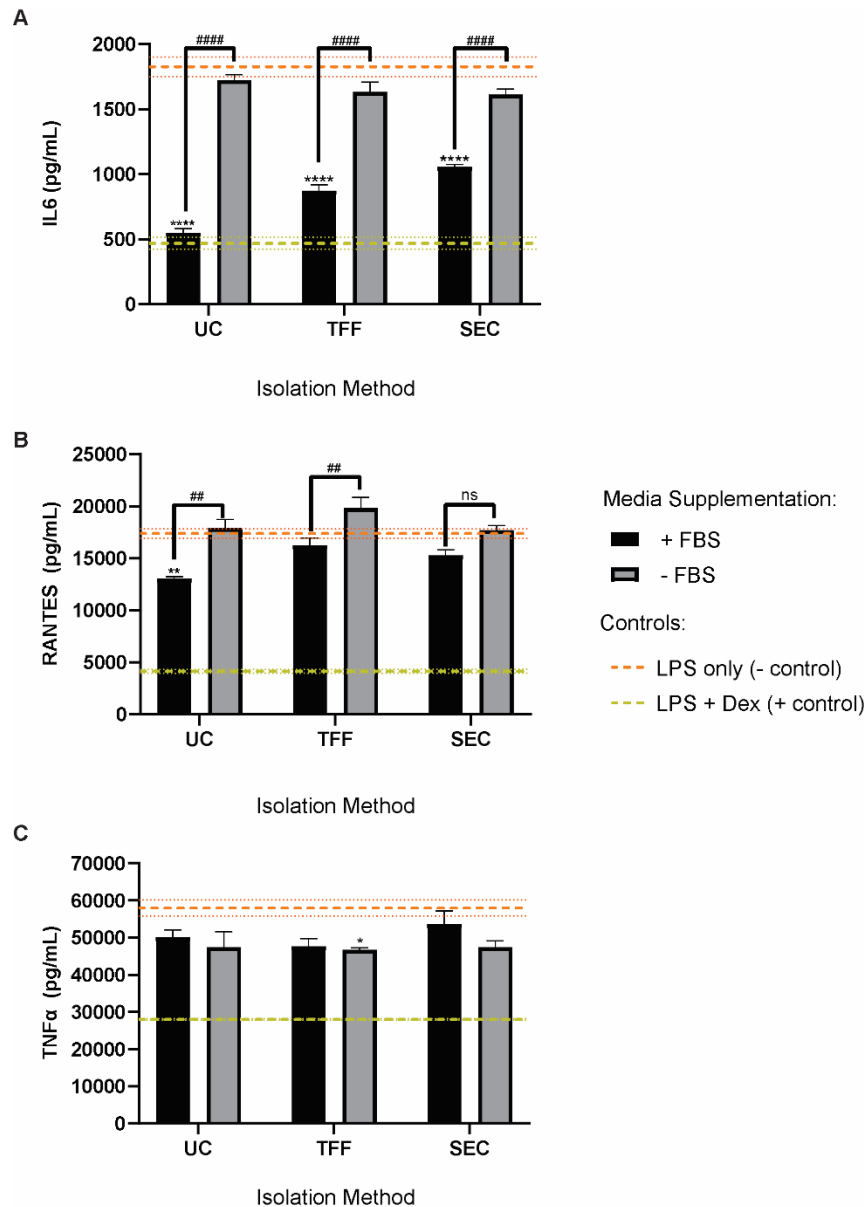
Figure 5. Fetal bovine serum (FBS) may be responsible for observed immunomodulatory responses of stimulated macrophages. Unconditioned media with FBS (+ FBS) and without FBS (-FBS) were subjected to a routine ultracentrifugation EV isolation protocol and applied to mouse macrophages prior to stimulation with LPS. The concentrations of (A) IL-6, (B) RANTES, and (C) TNF-α were quantified using ELISAs. Data is plotted as mean and error bars represent the standard error of the mean (SEM). Control means are represented as dashed lines with dotted lines representing the SEM. Data includes three technical replicates and data are representative of two independent biological replicates ($N = 2$). Statistical significance was calculated using a two-way ANOVA using Tukey's multiple comparison tests (ns – $p > 0.05$; *- $p < 0.05$; ** - $p < 0.01$; **** - $p < 0.0001$ compared to LPS negative control; #### - $p < 0.0001$).

23

458

459
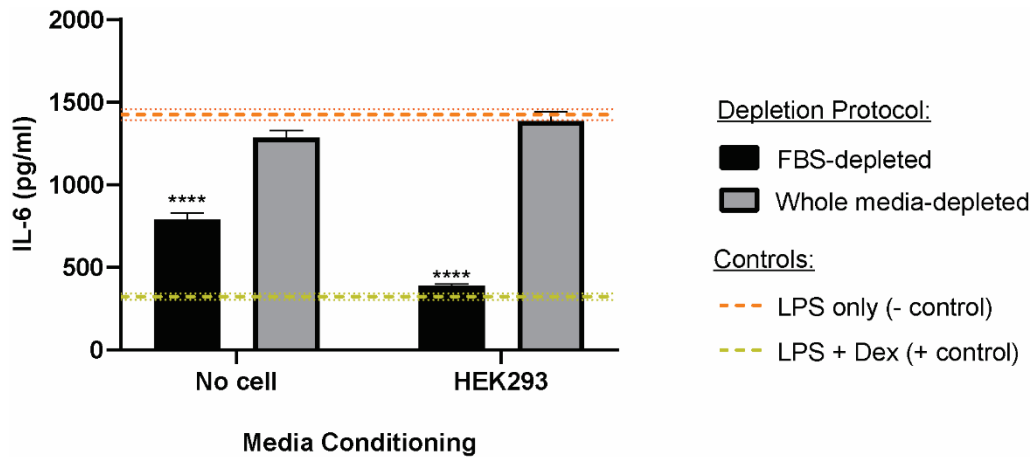
Figure 6. EV-depletion protocol of media supplements alter the results of the stimulated macrophage assay. FBS was either depleted of contaminating bovine EVs prior to addition to the media (FBS-depleted) or after addition (whole media-depletion), incubated either with (HEK293T) or without cells (no cell), subjected to the ultracentrifugation protocol, and applied to macrophages immediately prior to LPS. When the whole media protocol was used, IL-6 secretion was no longer suppressed. Data is plotted as mean and error bars represent the standard error of the mean (SEM). Control means are represented as dashed lines with dotted lines representing the SEM. Data includes three technical replicates and data are representative of two independent biological replicates ($N = 2$). Statistical significance was calculated using a two-way ANOVA using Tukey's multiple comparison tests (**** - $p < 0.0001$ compared to LPS negative control).

Discussion:

It is well-known that cell culture parameters (e.g., cell density, passage, media composition, substrate architecture) as well as isolation strategies can significantly impact the molecular composition and therapeutic function of EVs [16, 17, 31, 39-49]. Particularly, this has important downstream implications as movement from the bench to the clinic requires implementing scalable GMP-compliant manufacturing techniques in both EV production (e.g., serum-free media and dynamic bioreactors) and EV isolation (e.g., size-exclusion chromatography), which are often quite different from those utilized in the preclinical setting and can be ever-changing even through clinical phases [3]. In the present study, we set out to

24

482   investigate how these various upstream and downstream parameters may interact to alter EV

483   characteristics using HEK293T cells as the EV source based on the proven compatibility of these

484   cells with industry-scale bioprocess operations. To examine upstream parameters, we

485   implemented a 3D-printed scaffold-perfusion bioreactor system previously utilized in our lab and

486   exposed HEK293T cells to low levels of flow-derived shear stress (i.e., 3×10^{-3} dyn/cm^2). To

487   examine downstream isolation strategies, we isolated the subsequently secreted HEK293T EVs

488   using the gold-standard technique of ultracentrifugation (UC) and compared it with the more

489   scalable methods of size-exclusion chromatography (SEC) and tangential flow filtration (TFF).

490   Our results suggest that EV size and morphology are not significantly altered when these

491   particular cell culture parameters and isolation strategies are varied (**Figure 1**). It is important to

492   evaluate both EV size and shape as changes in these characteristics are used as indicators of EV

493   membrane integrity and have been known to be modified by external forces, particularly the

494   shearing involved in high-speed centrifugation [17, 40]. When coupled with membrane markers,

495   size can also be used to suggest possible EV biogenesis routes, as smaller EVs are thought to be

496   derived more so from the endosomal compartment rather than the plasma membrane [50].

497   Previous research has shown similar results in which EV size and shape are not changed by the

498   culture or isolation methodology used. For example, when comparing UC and TFF isolation

499   methods following traditional flask and 3D microcarrier bioreactor-based culture of umbilical

500   cord-derived MSCs, Haraszti and colleagues found all EV preparations to have similar size

501   distributions [16]. Additionally, prior work in our lab has demonstrated no significant effect of

502   dynamic culture on such physical parameters of EVs secreted from human dermal microvascular

503   endothelial cells (HDMECs) [5]. However, a study by Sharma et al. showed significant

504   differences in size distributions as well as nanoscale topography (i.e., surface roughness) that

505   was evident across various breast cancer cell-derived EVs that were isolated using four different

506   isolation methods (i.e., ultracentrifugation, density ultracentrifugation, immunoaffinity,

507   precipitation) [51]. The disagreement in results could be attributed to differences in assessment

508   techniques. While the aforementioned studies relied on nanoparticle tracking analysis and

509   transmission electron microscopy, Sharma and colleagues used disparate methods to quantify

510   and assess EV characteristics including atomic force microscopy (AFM), multi-angle light

511   scattering (MALS), direct stochastic optical reconstruction microscopy (dSTORM), and micro-

512   fluidic resistive pore sizing (MRPS). They also measured surface nano-roughness; a dimension

513   rarely evaluated for EVs [52]. Importantly, surface roughness of synthetic nanoparticles has been

514   proven to change the protein corona and subsequently alter their cellular uptake [53]. Although

515   of biological origin, it makes sense that alterations in the surface roughness of EVs may impart

516   similar changes in recipient cell internalization. Altogether these results suggest that, when

517   possible, it is important to utilize orthogonal methods and consider unique characteristics to more

518   rigorously assess EV biophysical parameters to help understand the mechanisms underlying

519   downstream therapeutic effects.

520   We then assessed whether the culture or isolation techniques alter the bioactivity of

521   HEK293T EVs by applying them in an *in vitro* LPS-stimulated mouse macrophage model. We

522   found that the EVs, particularly those isolated using ultracentrifugation, significantly reduced the

523   secretion of pro-inflammatory cytokines (i.e., IL-6 and RANTES); an effect that was largely lost

524   when culturing within the bioreactor or isolating using TFF or SEC (**Figure 2**). As HEK293T

525   EVs are not known to have significant immunomodulatory effects [34], these results were

526   unexpected. Nevertheless, ultracentrifugation is notorious for the co-isolation of proteins and

527   other small molecules which may be imparting the observed therapeutic effect [51, 54-56].

528 Moreover, previous research in our lab using a similar bioreactor has shown a significant

529 reduction in total protein content per EV [5], which could help explain the loss of the observed

530 effect when using EVs from HEK293T cells cultured within the bioreactor in the present study

531 (**Figure 2**). This change in protein content in dynamic culture is to be expected as it has been

532 shown that flow can alter the protein corona that forms on nanoparticles [57]. The composition

533 of the EV protein corona under dynamic conditions should be evaluated in future studies.

534   To confirm whether the HEK293T EVs themselves were truly suppressing cytokine

535 secretion, we focused only on traditional flask culture and assessed the effect of unconditioned

536 media (i.e., media incubated without cells) after being processed using UC, TFF, and SEC. We

537 found that the unconditioned media significantly reduced the IL-6 concentration regardless of

538 isolation technique and lessened the RANTES and TNF-α concentrations particularly when

539 isolating using UC and TFF, respectively (**Figure 3**). We found that this observation of the

540 unconditioned media having an effect was only present in this specific assay, as there were no

541 significant effects of unconditioned media subjected to ultracentrifugation in other *in vitro* assays

542 commonly used to assess EV bioactivity (i.e., gap closure and tube formation) (**Figure 4**). This

543 suggests an interaction between the component(s) of the media and the LPS response in this

544 particular assay. Indeed, fetal bovine serum (FBS), a common reagent for media

545 supplementation, has been shown to alter LPS sensitivity in cell cultures [58] as well alter EV

546 analyses [59]. Thus, we tested unconditioned media without FBS supplementation and found that

547 nearly all treatments were comparable to the LPS control, thus implicating FBS as the

548 component responsible for the cytokine suppression (**Figure 5**). Interestingly, a previous study

549 by Beninson and Fleshner found that FBS-derived EVs can have an immunosuppressive effect

550 on primary rat macrophages [60]. Inspired by this, we revisited our EV-depletion protocol and

551   found that differences in the methodology used to EV-deplete media can result in drastic

552   differences in cytokine secretion (**Figure 6**). In the pursuit of understanding the effects of

553   HEK293T EVs in the stimulated macrophage model, we were able to optimize our existing EV-

554   depletion protocol which is a foundational component of the majority of our research.

555   As EV-based therapies have shown promise in a wide array of applications, there is much

556   interest in the movement of these therapeutics into the clinic. However, successful clinical

557   translation hinges upon the ability to optimize EV therapeutic effects within a scalable, GMP-

558   compliant environment. In our work, we demonstrate an unexpected immunosuppressive effect

559   of HEK293T EVs that differed depending on culture conditions of the HEK293T cells as well as

560   isolation strategies used for the EVs. This may explain the disparity between studies that report

561   no effect of unmodified HEK293T EVs in their bioactivity assays [61, 62] and others that

562   describe significant immunomodulatory activity [63]. As some culture conditions and isolation

563   methods may be more amenable to scale-up processes than others, it is important to consider

564   these parameters as early as possible to ensure a smooth transition to clinical exploration. We

565   also show that media components from the cell culture may contaminate the separated

566   formulation and alter final EV therapeutic evaluation; a result that further emphasizes the

567   urgency to move to xeno-free, chemically-defined culture conditions and to improve or introduce

568   new downstream separation methods. As identity and purity are major quality considerations to

569   move investigative new drugs into the realm of approved therapeutics [3], this work reiterates the

570   necessity for multiple orthogonal assays as well as the consideration of all controls in order to

571   confirm that any observed effects are truly the result of the experimental EV condition.

572

573

580   **Literature Cited:**

581   [1] K. O'Brien, K. Breyne, S. Ughetto, L.C. Laurent, X.O. Breakefield, RNA delivery by
582   extracellular vesicles in mammalian cells and its applications, Nat Rev Mol Cell Biol 21(10)
583   (2020) 585-606.
584   [2] G. van Niel, G. D'Angelo, G. Raposo, Shedding light on the cell biology of extracellular
585   vehicles, 2017.
586   [3] E. Rohde, K. Pachler, M. Gimona, Manufacturing and characterization of extracellular
587   vesicles from umbilical cord-derived mesenchymal stromal cells for clinical testing, Cytotherapy
588   21(6) (2019) 581-592.
589   [4] S. Thippabhotla, C. Zhong, M. He, 3D cell culture stimulates the secretion of in vivo like
590   extracellular vesicles, Sci Rep 9(1) (2019) 13012.
591   [5] D.B. Patel, C.R. Luthers, M.J. Lerman, J.P. Fisher, S.M. Jay, Enhanced extracellular vesicle
592   production and ethanol-mediated vascularization bioactivity via a 3D-printed scaffold-perfusion
593   bioreactor system, Acta Biomater 95 (2019) 236-244.
594   [6] D.C. Watson, D. Bayik, A. Srivatsan, C. Bergamaschi, A. Valentin, G. Niu, J. Bear, M.
595   Monninger, M. Sun, A. Morales-Kastresana, J.C. Jones, B.K. Felber, X. Chen, I. Gursel, G.N.
596   Pavlakis, Efficient production and enhanced tumor delivery of engineered extracellular vesicles,
597   Biomaterials 105 (2016) 195-205.
598   [7] M. de Almeida Fuzeta, N. Bernardes, F.D. Oliveira, A.C. Costa, A. Fernandes-Platzgummer,
599   J.P. Farinha, C.A.V. Rodrigues, S. Jung, R.J. Tseng, W. Milligan, B. Lee, M. Castanho, D.
600   Gaspar, J.M.S. Cabral, C.L. da Silva, Scalable Production of Human Mesenchymal Stromal Cell-
601   Derived Extracellular Vesicles Under Serum-/Xeno-Free Conditions in a Microcarrier-Based
602   Bioreactor Culture System, Front Cell Dev Biol 8 (2020) 553444.
603   [8] J. Gobin, G. Muradia, J. Mehic, C. Westwood, L. Couvrette, A. Stalker, S. Bigelow, C.C.
604   Luebbert, F.S. Bissonnette, M.J.W. Johnston, S. Sauve, R.Y. Tam, L. Wang, M. Rosu-Myles,
605   J.R. Lavoie, Hollow-fiber bioreactor production of extracellular vesicles from human bone
606   marrow mesenchymal stromal cells yields nanovesicles that mirrors the immuno-modulatory
607   antigenic signature of the producer cell, Stem Cell Res Ther 12(1) (2021) 127.
608   [9] S. Guo, L. Debbi, B. Zohar, R. Samuel, R.S. Arzi, A.I. Fried, T. Carmon, D. Shevach, I.
609   Redenski, I. Schlachet, A. Sosnik, S. Levenberg, Stimulating Extracellular Vesicles Production
610   from Engineered Tissues by Mechanical Forces, Nano Lett 21(6) (2021) 2497-2504.
611   [10] R. Jeske, C. Liu, L. Duke, M.L. Canonicco Castro, L. Muok, P. Arthur, M. Singh, S. Jung,
612   L. Sun, Y. Li, Upscaling human mesenchymal stromal cell production in a novel vertical-wheel
613   bioreactor enhances extracellular vesicle secretion and cargo profile, Bioactive Materials (2022).

614 [11] J. Phelps, C. Leonard, S. Shah, R. Krawetz, D.A. Hart, N.A. Duncan, A. Sen, Production of
615 Mesenchymal Progenitor Cell-Derived Extracellular Vesicles in Suspension Bioreactors for Use
616 in Articular Cartilage Repair, Stem Cells Transl Med 11(1) (2022) 73-87.
617 [12] H. Kang, Y.H. Bae, Y. Kwon, S. Kim, J. Park, Extracellular Vesicles Generated Using
618 Bioreactors and their Therapeutic Effect on the Acute Kidney Injury Model, Adv Healthc Mater
619 11(4) (2022) e2101606.
620 [13] J. Wu, D. Wu, G. Wu, H.P. Bei, Z. Li, H. Xu, Y. Wang, D. Wu, H. Liu, S. Shi, C. Zhao, Y.
621 Xu, Y. He, J. Li, C. Wang, X. Zhao, S. Wang, Scale-out production of extracellular vesicles
622 derived from natural killer cells via mechanical stimulation in a seesaw-motion bioreactor for
623 cancer therapy, Biofabrication 14(4) (2022).
624 [14] J. Cao, B. Wang, T. Tang, L. Lv, Z. Ding, Z. Li, R. Hu, Q. Wei, A. Shen, Y. Fu, B. Liu,
625 Three-dimensional culture of MSCs produces exosomes with improved yield and enhanced
626 therapeutic efficacy for cisplatin-induced acute kidney injury, Stem Cell Res Ther 11(1) (2020)
627 206.
628 [15] A. Jarmalaviciute, V. Tunaitis, U. Pivoraite, A. Venalis, A. Pivoriunas, Exosomes from
629 dental pulp stem cells rescue human dopaminergic neurons from 6-hydroxy-dopamine-induced
630 apoptosis, Cytotherapy 17(7) (2015) 932-9.
631 [16] R.A. Haraszti, R. Miller, M. Stoppato, Y.Y. Sere, A. Coles, M.C. Didiot, R. Wollacott, E.
632 Sapp, M.L. Dubuke, X. Li, S.A. Shaffer, M. DiFiglia, Y. Wang, N. Aronin, A. Khvorova,
633 Exosomes Produced from 3D Cultures of MSCs by Tangential Flow Filtration Show Higher
634 Yield and Improved Activity, Mol Ther 26(12) (2018) 2838-2847.
635 [17] E.A. Mol, M.J. Goumans, P.A. Doevendans, J.P.G. Sluijter, P. Vader, Higher functionality
636 of extracellular vesicles isolated using size-exclusion chromatography compared to
637 ultracentrifugation, Nanomedicine 13(6) (2017) 2061-2065.
638 [18] A.C. Andrade, M. Wolf, H.M. Binder, F.G. Gomes, F. Manstein, P. Ebner-Peking, R.
639 Poupardin, R. Zweigerdt, K. Schallmoser, D. Strunk, Hypoxic Conditions Promote the
640 Angiogenic Potential of Human Induced Pluripotent Stem Cell-Derived Extracellular Vesicles,
641 Int J Mol Sci 22(8) (2021).
642 [19] M. Popović, A. de Marco, Canonical and selective approaches in exosome purification and
643 their implications for diagnostic accuracy, Translational Cancer Research 7(S2) (2018) S209-
644 S225.
645 [20] T.E. Whittaker, A. Nagelkerke, V. Nele, U. Kauscher, M.M. Stevens, Experimental artefacts
646 can lead to misattribution of bioactivity from soluble mesenchymal stem cell paracrine factors to
647 extracellular vesicles, J Extracell Vesicles 9(1) (2020) 1807674.
648 [21] D. Furman, J. Campisi, E. Verdin, P. Carrera-Bastos, S. Targ, C. Franceschi, L. Ferrucci,
649 D.W. Gilroy, A. Fasano, G.W. Miller, A.H. Miller, A. Mantovani, C.M. Weyand, N. Barzilai,
650 J.J. Goronzy, T.A. Rando, R.B. Effros, A. Lucia, N. Kleinstreuer, G.M. Slavich, Chronic
651 inflammation in the etiology of disease across the life span, Nat Med 25(12) (2019) 1822-1832.
652 [22] R. Zhao, H. Liang, E. Clarke, C. Jackson, M. Xue, Inflammation in Chronic Wounds, Int J
653 Mol Sci 17(12) (2016).
654 [23] N. Pacienza, R.H. Lee, E.H. Bae, D.K. Kim, Q. Liu, D.J. Prockop, G. Yannarelli, In Vitro
655 Macrophage Assay Predicts the In Vivo Anti-inflammatory Potential of Exosomes from Human
656 Mesenchymal Stromal Cells, Mol Ther Methods Clin Dev 13 (2019) 67-76.
657 [24] Y. Kuwahara, K. Yoshizaki, H. Nishida, H. Kamishina, S. Maeda, K. Takano, N. Fujita, R.
658 Nishimura, J.I. Jo, Y. Tabata, H. Akiyoshi, Extracellular Vesicles Derived From Canine

659 Mesenchymal Stromal Cells in Serum Free Culture Medium Have Anti-inflammatory Effect on
660 Microglial Cells, Front Vet Sci 8 (2021) 633426.
661 [25] R. Malvicini, D. Santa-Cruz, G. De Lazzari, A.M. Tolomeo, C. Sanmartin, M. Muraca, G.
662 Yannarelli, N. Pacienza, Macrophage bioassay standardization to assess the anti-inflammatory
663 activity of mesenchymal stromal cell-derived small extracellular vesicles, Cytotherapy (2022).
664 [26] Z. Wang, K. Maruyama, Y. Sakisaka, S. Suzuki, H. Tada, M. Suto, M. Saito, S. Yamada, E.
665 Nemoto, Cyclic Stretch Force Induces Periodontal Ligament Cells to Secrete Exosomes That
666 Suppress IL-1beta Production Through the Inhibition of the NF-kappaB Signaling Pathway in
667 Macrophages, Front Immunol 10 (2019) 1310.
668 [27] J. Kim, Y. Song, C.H. Park, C. Choi, Platform technologies and human cell lines for the
669 production of therapeutic exosomes, Extracellular Vesicles and Circulating Nucleic Acids
670 (2021).
671 [28] L.J. Born, K.H. Chang, P. Shoureshi, F. Lay, S. Bengali, A.T.W. Hsu, S.N. Abadchi, J.W.
672 Harmon, S.M. Jay, HOTAIR-Loaded Mesenchymal Stem/Stromal Cell Extracellular Vesicles
673 Enhance Angiogenesis and Wound Healing, Adv Healthc Mater (2021) e2002070.
674 [29] A.E. Pottash, D. Levy, A. Jeyaram, L. Kuo, S.M. Kronstadt, W. Chao, S.M. Jay,
675 Combinatorial microRNA Loading into Extracellular Vesicles for Anti-Inflammatory Therapy,
676 BioRxiv (2022).
677 [30] D. Levy, A. Jeyaram, L.J. Born, K.-H. Chang, S.N. Abadchi, A.T. Wei Hsu, T. Solomon, A.
678 Aranda, S. Stewart, X. He, J.W. Harmon, S.M. Jay, The Impact of Storage Condition and
679 Duration on Function of Native and Cargo-Loaded Mesenchymal Stromal Cell Extracellular
680 Vesicles, BioRxiv (2022).
681 [31] D.B. Patel, K.M. Gray, Y. Santharam, T.N. Lamichhane, K.M. Stroka, S.M. Jay, Impact of
682 cell culture parameters on production and vascularization bioactivity of mesenchymal stem cell-
683 derived extracellular vesicles, Bioeng Transl Med 2(2) (2017) 170-179.
684 [32] J.M. Gudbergsson, K.B. Johnsen, M.N. Skov, M. Duroux, Systematic review of factors
685 influencing extracellular vesicle yield from cell cultures, Cytotechnology 68(4) (2016) 579-92.
686 [33] E. Tan, C.S.H. Chin, Z.F.S. Lim, S.K. Ng, HEK293 Cell Line as a Platform to Produce
687 Recombinant Proteins and Viral Vectors, Front Bioeng Biotechnol 9 (2021) 796991.
688 [34] X. Zhu, M. Badawi, S. Pomeroy, D.S. Sutaria, Z. Xie, A. Baek, J. Jiang, O.A. Elgamal, X.
689 Mo, K. Perle, J. Chalmers, T.D. Schmittgen, M.A. Phelps, Comprehensive toxicity and
690 immunogenicity studies reveal minimal effects in mice following sustained dosing of
691 extracellular vesicles derived from HEK293T cells, J Extracell Vesicles 6(1) (2017) 1324730.
692 [35] A.F. Saleh, E. Lázaro-Ibáñez, M.A.M. Forsgard, O. Shatnyeva, X. Osteikoetxea, F.
693 Karlsson, N. Heath, M. Ingelsten, J. Rose, J. Harris, M. Mairesse, S.M. Bates, M. Clausen, D.
694 Etal, E. Leonard, M.D. Fellows, N. Dekker, N. Edmunds, Extracellular vesicles induce minimal
695 hepatotoxicity and immunogenicity, Nanoscale 11(14) (2019) 6990-7001.
696 [36] Y. Zhang, Z. Hao, P. Wang, Y. Xia, J. Wu, D. Xia, S. Fang, S. Xu, Exosomes from human
697 umbilical cord mesenchymal stem cells enhance fracture healing through HIF-1alpha-mediated
698 promotion of angiogenesis in a rat model of stabilized fracture, Cell Prolif 52(2) (2019) e12570.
699 [37] S. Ahmadvand Koohsari, A. Absalan, D. Azadi, Human umbilical cord mesenchymal stem
700 cell-derived extracellular vesicles attenuate experimental autoimmune encephalomyelitis via
701 regulating pro and anti-inflammatory cytokines, Sci Rep 11(1) (2021) 11658.
702 [38] F.F. Cruz, Z.D. Borg, M. Goodwin, D. Sokocevic, D.E. Wagner, A. Coffey, M. Antunes,
703 K.L. Robinson, S.A. Mitsialis, S. Kourembanas, K. Thane, A.M. Hoffman, D.H. McKenna, P.R.
704 Rocco, D.J. Weiss, Systemic Administration of Human Bone Marrow-Derived Mesenchymal

Stromal Cell Extracellular Vesicles Ameliorates Aspergillus Hyphal Extract-Induced Allergic Airway Inflammation in Immunocompetent Mice, Stem Cells Transl Med 4(11) (2015) 1302-16.

[39] D.B. Patel, M. Santoro, L.J. Born, J.P. Fisher, S.M. Jay, Towards rationally designed biomanufacturing of therapeutic extracellular vesicles: impact of the bioproduction microenvironment, Biotechnol Adv 36(8) (2018) 2051-2059.

[40] D.D. Taylor, S. Shah, Methods of isolating extracellular vesicles impact down-stream analyses of their cargoes, Methods 87 (2015) 3-10.

[41] D. Buschmann, B. Kirchner, S. Hermann, M. Marte, C. Wurmser, F. Brandes, S. Kotschote, M. Bonin, O.K. Steinlein, M.W. Pfaffl, G. Schelling, M. Reithmair, Evaluation of serum extracellular vesicle isolation methods for profiling miRNAs by next-generation sequencing, J Extracell Vesicles 7(1) (2018) 1481321.

[42] J.M. Gudbergsson, K. Jonsson, J.B. Simonsen, K.B. Johnsen, Systematic review of targeted extracellular vesicles for drug delivery - Considerations on methodological and biological heterogeneity, J Control Release 306 (2019) 108-120.

[43] C.N. Davis, H. Phillips, J.J. Tomes, M.T. Swain, T.J. Wilkinson, P.M. Brophy, R.M. Morphew, The importance of extracellular vesicle purification for downstream analysis: A comparison of differential centrifugation and size exclusion chromatography for helminth pathogens, PLoS Negl Trop Dis 13(2) (2019) e0007191.

[44] G.K. Patel, M.A. Khan, H. Zubair, S.K. Srivastava, M. Khushman, S. Singh, A.P. Singh, Comparative analysis of exosome isolation methods using culture supernatant for optimum yield, purity and downstream applications, Sci Rep 9(1) (2019) 5335.

[45] J. Van Deun, P. Mestdagh, R. Sormunen, V. Cocquyt, K. Vermaelen, J. Vandesompele, M. Bracke, O. De Wever, A. Hendrix, The impact of disparate isolation methods for extracellular vesicles on downstream RNA profiling, J Extracell Vesicles 3 (2014).

[46] M. Palviainen, H. Saari, O. Karkkainen, J. Pekkinen, S. Auriola, M. Yliperttula, M. Puhka, K. Hanhineva, P.R. Siljander, Metabolic signature of extracellular vesicles depends on the cell culture conditions, J Extracell Vesicles 8(1) (2019) 1596669.

[47] Y. Zhang, M. Chopp, Z.G. Zhang, M. Katakowski, H. Xin, C. Qu, M. Ali, A. Mahmood, Y. Xiong, Systemic administration of cell-free exosomes generated by human bone marrow derived mesenchymal stem cells cultured under 2D and 3D conditions improves functional recovery in rats after traumatic brain injury, Neurochem Int 111 (2017) 69-81.

[48] C.Y. Ng, L.T. Kee, M.E. Al-Masawa, Q.H. Lee, T. Subramaniam, D. Kok, M.H. Ng, J.X. Law, Scalable Production of Extracellular Vesicles and Its Therapeutic Values: A Review, Int J Mol Sci 23(14) (2022).

[49] D. Freitas, M. Balmana, J. Pocas, D. Campos, H. Osorio, A. Konstantinidi, S.Y. Vakhrushev, A. Magalhaes, C.A. Reis, Different isolation approaches lead to diverse glycosylated extracellular vesicle populations, J Extracell Vesicles 8(1) (2019) 1621131.

[50] M. Tkach, J. Kowal, C. Thery, Why the need and how to approach the functional diversity of extracellular vesicles, Philos Trans R Soc Lond B Biol Sci 373(1737) (2018).

[51] S. Sharma, M. LeClaire, J. Wohlschlegel, J. Gimzewski, Impact of isolation methods on the biophysical heterogeneity of single extracellular vesicles, Sci Rep 10(1) (2020) 13327.

[52] J. Woo, S. Sharma, J. Gimzewski, The Role of Isolation Methods on a Nanoscale Surface Structure and its Effect on the Size of Exosomes, J Circ Biomark 5 (2016) 11.

[53] A. Piloni, C.K. Wong, F. Chen, M. Lord, A. Walther, M.H. Stenzel, Surface roughness influences the protein corona formation of glycosylated nanoparticles and alter their cellular uptake, Nanoscale 11(48) (2019) 23259-23267.

751 [54] S.M. Langevin, D. Kuhnell, M.A. Orr-Asman, J. Biesiada, X. Zhang, M. Medvedovic, H.E.
752 Thomas, Balancing yield, purity and practicality: a modified differential ultracentrifugation
753 protocol for efficient isolation of small extracellular vesicles from human serum, RNA Biol
754 16(1) (2019) 5-12.
755 [55] J.B. Simonsen, What Are We Looking At? Extracellular Vesicles, Lipoproteins, or Both?,
756 Circ Res 121(8) (2017) 920-922.
757 [56] M. Auber, D. Frohlich, O. Drechsel, E. Karaulanov, E.M. Kramer-Albers, Serum-free media
758 supplements carry miRNAs that co-purify with extracellular vesicles, J Extracell Vesicles 8(1)
759 (2019) 1656042.
760 [57] D.T. Jayaram, S.M. Pustulka, R.G. Mannino, W.A. Lam, C.K. Payne, Protein Corona in
761 Response to Flow: Effect on Protein Concentration and Structure, Biophys J 115(2) (2018) 209-
762 216.
763 [58] N. Yang, D.D. Sin, D.R. Dorscheid, Various Factors Affect Lipopolysaccharide
764 Sensitization in Cell Cultures, BioTechniques 69 (2020) 127-132.
765 [59] B.M. Lehrich, Y. Liang, M.S. Fiandaca, Foetal bovine serum influence on in vitro
766 extracellular vesicle analyses, J Extracell Vesicles 10(3) (2021) e12061.
767 [60] L.A. Beninson, M. Fleshner, Exosomes in fetal bovine serum dampen primary macrophage
768 IL-1beta response to lipopolysaccharide (LPS) challenge, Immunol Lett 163(2) (2015) 187-92.
769 [61] A. Jeyaram, T.N. Lamichhane, S. Wang, L. Zou, E. Dahal, S.M. Kronstadt, D. Levy, B.
770 Parajuli, D.R. Knudsen, W. Chao, S.M. Jay, Enhanced Loading of Functional miRNA Cargo via
771 pH Gradient Modification of Extracellular Vesicles, Mol Ther 28(3) (2020) 975-985.
772 [62] T.N. Lamichhane, A. Jeyaram, D.B. Patel, B. Parajuli, N.K. Livingston, N. Arumugasaamy,
773 J.S. Schardt, S.M. Jay, Oncogene Knockdown via Active Loading of Small RNAs into
774 Extracellular Vesicles by Sonication, Cell Mol Bioeng 9(3) (2016) 315-324.
775 [63] H. Choi, Y. Kim, A. Mirzaaghasi, J. Heo, Y.N. Kim, J.H. Shin, S. Kim, N.H. Kim, E.S.
776 Cho, J. In Yook, T.H. Yoo, E. Song, P. Kim, E.C. Shin, K. Chung, K. Choi, C. Choi, Exosome-
777 based Delivery of Super-Repressor IkBa Relieves Sepsis-Associated Organ Damage and
778 Mortality Science Advances 6(15) (2020).

779